Journal of Computational Physics 229 (2010) 7162–7179

Contents lists available at ScienceDirect

Journal of Computational Physics

journal homepage: www.elsevier.com/locate/jcp

Numerical method for solving matrix coefficient elliptic equation with sharp-edged interfaces

Songming Hou *, Wei Wang, Liqun Wang

Dept. of Mathematics and Statistics, Louisiana Tech University, Ruston, LA 71272, United States

ARTICLE INFO

Article history:
Received 19 October 2009
Received in revised form 12 March 2010
Accepted 2 June 2010
Available online 19 June 2010

Keywords:
Elliptic equation
Sharp-edged interface
Jump condition
Matrix coefficient

ABSTRACT

Solving elliptic equations with sharp-edged interfaces is a challenging problem for most existing methods, especially when the solution is highly oscillatory. Nonetheless, it has wide applications in engineering and science. An accurate and efficient method is desired. We propose an efficient non-traditional finite element method with non-body-fitting grids to solve the matrix coefficient elliptic equations with sharp-edged interfaces. Extensive numerical experiments show that this method is second order accurate in the L^∞ norm and that it can handle both sharp-edged interface and oscillatory solutions.

Published by Elsevier Inc.

1. Introduction

The importance of elliptic interface problems has been well recognized in a variety of disciplines, such as electromagnetics, material science, fluid dynamics and so on. However, designing highly efficient methods for these problems is a difficult job because of the low global regularity of the solution. Since 1977, after the pioneering work of Peskin [14], much attention has been paid to the numerical solution of elliptic equations with discontinuous coefficients and singular sources on regular Cartesian grids. In many studies, simple Cartesian grids are preferred. In this way, the complicated procedure of generating an unstructured grid can be bypassed, and we can use well developed fast algebraic solvers.

The "immersed boundary" method [14,15] uses a numerical approximation of the δ-function, which smears out the solution on a thin finite band around the interface Γ. In [16], the "immersed boundary" method was combined with the level-set method, resulting in a first order numerical method that is simple to implement, even in multiple spatial dimensions. However, for both methods, the numerical smearing at the interface forces continuity of the solution at the interface, regardless of the interface condition $[u] = a$, where a might not be zero.

In [11,12], a fast method for solving Laplace's equations on irregular regions with smooth boundaries was introduced. By using Fredholm integral equations of the second kind, solutions can be extended to a rectangular region. Since solutions are harmonic, Fredholm integral equations can be used to capture the jump conditions in the solution and its normal derivative, $[u] \neq 0$ and $[u_n] = 0$. Then these jump conditions are used to evaluate the discrete Laplacian, and then a fast Poisson solver on a regular region can be applied with second or higher order accuracy.

In [5], the "immersed interface" method was presented. This method achieves second order accuracy by incorporating the interface conditions into the finite difference stencil in a way that preserves the interface conditions in both solution and its co-normal derivative, $[u] \neq 0$ and $[\beta u_n] \neq 0$. The corresponding linear system is sparse, but not symmetric or positive definite. Various applications and extensions of the "immersed interface" method are discussed in [8].

* Corresponding author.
E-mail addresses: shou@latech.edu (S. Hou), htprww@gmail.com (W. Wang), wliqunhmily@gmail.com (L. Wang).

0021-9991/$ - see front matter Published by Elsevier Inc.
doi:10.1016/j.jcp.2010.06.005

In [20], a finite element method was developed for solving elliptic problems with the interface conditions $[u] = 0$ and $[\beta u_n] \neq 0$. Interfaces are aligned with cell boundaries. Second order accuracy was obtained in an energy norm. Nearly second order accuracy was obtained in the L^2 norm.

In [6], a fast iterative method in conjunction with the "immersed interface" method has been developed for constant coefficient problems with the interface conditions $[u] = 0$ and $[\beta u_n] \neq 0$. Non-body-fitting Cartesian grids are used, and then associated uniform triangulations are added on. Interfaces are not necessarily aligned with cell boundaries. Numerical evidence shows that this method's conforming version achieves second order accuracy in the L^∞ norm, and higher than first order for its non-conforming version.

The boundary condition capturing method [9] uses the Ghost fluid method (GFM) [2] to capture the boundary conditions. The GFM is robust and simple to implement, and so is the resulting boundary condition capturing method. The boundary condition capturing method has been sped up by a multi-grid method [17]. The convergence proof for the method is provided in [10]. The boundary condition capturing method can be obtained from discretizing the weak formulation provided in [10]. The convergence proof follows naturally. The method can solve the elliptic equation with interface conditions $[u] \neq 0$ and $[\beta u_n] \neq 0$ in two and three dimensions. However, the original version is only first order accurate. In a recent work [25], the method is improved to second order accuracy for smooth interfaces.

In [4], a non-traditional finite element formulation for solving elliptic equations with smooth or sharp-edged interfaces was proposed with non-body-fitting grids for $[u] \neq 0$ and $[\beta u_n] \neq 0$. It achieved second order accuracy in the L^∞ norm for smooth interfaces and about 0.8th order for sharp-edged interfaces. In [21], the matched interface and boundary (MIB) method was proposed to solve elliptic equations with smooth interfaces. In [19], the MIB method was generalized to treat sharp-edged interfaces. With an elegant treatment, second order accuracy was achieved in the L^∞ norm. However, for oscillatory solutions, the errors degenerate. Also, there has been a large body of work from the finite volume perspective for developing high order methods for elliptic equations in complex domains, such as [22,23] for two dimensional problems and [24] for three dimensional problems. Another recent work in this area is a class of kernel-free boundary integral (KFBI) methods for solving elliptic BVPs, presented in [18].

In this paper, inspired by the boundary condition capturing method [9] and the weak formulation derived in [10], we further generalize the method introduced in [4]. We use a finite element formulation for solving elliptic equations with sharp-edged interfaces with β being uniformly elliptic (therefore, positive definite) and lower order terms present. We provided proofs for the generalized version of the theorems in [10], and we proved the resulting linear system is (unsymmetric) positive definite if β is positive definite and lower order terms are not present. We also provided extensive numerical experiments. Compared with the previous work in [4], we improved the order of accuracy for sharp-edged interface from 0.8th to close to second order, see Example 4. Compared with the results in [19], the more oscillatory the solution is, the more advantageous our method is, see Examples 1–3. The orders of accuracy for different regularity of solutions and different regularity of the interface are listed in Table 11.

2. Equations and weak formulation

Consider an open bounded domain $\Omega \subset R^d$. Let Γ be an interface of co-dimension $d-1$, which divides Ω into disjoint open subdomains, Ω^- and Ω^+, hence $\Omega = \Omega^- \bigcup \Omega^+ \bigcup \Gamma$. Assume that the boundary $\partial\Omega$ and the boundary of each subdomain $\partial\Omega^\pm$ are Lipschitz continuous as submanifolds. Since $\partial\Omega^\pm$ are Lipschitz continuous, so is Γ. A unit normal vector of Γ can be defined a.e. on Γ, see Section 1.5 in [3].

We seek solutions of the variable coefficient elliptic equation away from the interface Γ given by

$$-\bigtriangledown\cdot(\beta(x)\bigtriangledown u(x)) + p(x)\cdot\bigtriangledown u(x) + q(x)u(x) = f(x), \quad x \in \Omega\setminus\Gamma \tag{1}$$

in which $x = (x_1,\ldots,x_d)$ denotes the spatial variables and $\bigtriangledown$ is the gradient operator. The coefficient $\beta(x)$ is assumed to be a $d\times d$ matrix that is uniformly elliptic on each disjoint subdomain, Ω^- and Ω^+, and its components are continuously differentiable on each disjoint subdomain, but they may be discontinuous across the interface Γ. The right-hand side $f(x)$ is assumed to lie in $L^2(\Omega)$.

Given functions a and b along the interface Γ, we prescribe the jump conditions

$$\begin{cases} [u]_\Gamma(x) \equiv u^+(x) - u^-(x) = a(x) \\ [(\beta\bigtriangledown u)\cdot n]_\Gamma(x) \equiv n\cdot(\beta^+(x)\bigtriangledown u^+(x)) - n\cdot(\beta^-(x)\bigtriangledown u^-(x)) = b(x) \end{cases} \tag{2}$$

The "±" superscripts refer to limits taken from within the subdomains $\Omega^\pm$.

Finally, we prescribe boundary conditions

$$u(x) = g(x), \quad x \in \partial\Omega \tag{3}$$

for a given function g on the boundary $\partial\Omega$.

We generalize the weak formulation in [4] for the elliptic equation with matrix coefficient and lower order terms present. We are going to use the usual Sobolev spaces $H^1(\Omega)$. For $H_0^1(\Omega)$, instead of the usual inner product we choose one which is better suited to our problem:

$$B[u,v]=\int_{\Omega^+}\beta\bigtriangledown u\cdot\bigtriangledown v+\int_{\Omega^-}\beta\bigtriangledown u\cdot\bigtriangledown v+\int_{\Omega^+}(p\cdot\bigtriangledown u)v+\int_{\Omega^-}(p\cdot\bigtriangledown u)v+\int_{\Omega^+}quv+\int_{\Omega^-}quv \tag{4}$$

Remark. For general second order elliptic equations with lower order p,q terms, one of the hypotheses of the Lax–Milgram Theorem is not guaranteed. For detailed discussion about the energy estimates and a first existence theorem for weak solutions, see [1]. Although we provide a numerical example with $p\neq 0$, $q\neq 0$ in Section 4, for ease of theoretical discussion, we assume $p=0$, $q=0$ for the rest of this section as well as in the next section.

Eq. (4) without the p, q terms induces a norm on $H_0^1(\Omega)$ which is equivalent to the usual one, thanks to the Poincare inequality and the uniformly ellipticity and boundedness of $\beta(x)$ on Ω.

Let Γ be any closed Lipschitz continuous hyper-surface of dimension $d-1$ in $\overline{\Omega}$, where the overline denotes the closure of a set. Let R denote the restriction operator from $H^1(\Omega)$ to $L^2(\partial\Omega^-)$. This restriction operator R is well defined and bounded, because it is closed Lipschitz continuous (see Theorem 2.4.2 in [13]) and $C^1(\overline{\Omega})$ is dense in $H^1(\Omega)$. Throughout this section, we shall always assume that our interface data a and b are the restrictions of functions $\tilde{a}$ and $\tilde{b}\in H^1(\Omega)$ on $\partial\Omega^-$ and then limited on Γ, respectively. That is on Γ,

$$a=R_{\partial\Omega^-}(\tilde{a}),\quad b=R_{\partial\Omega^-}(\tilde{b}) \tag{5}$$

We shall always assume that our boundary data g can be obtained: Assume that there exist a function $\tilde{c}\in H^1(\Omega)$ so that g is given as, on $\partial\Omega$,

$$g=\begin{cases}R_{\partial\Omega}(\tilde{c}-\tilde{a}), & \text{on}\quad \partial\Omega\bigcap\partial\Omega^-\\ R_{\partial\Omega}(\tilde{c}), & \text{on}\quad \partial\Omega\setminus\partial\Omega^-\end{cases} \tag{6}$$

Eq. (6) could be thought as a compatibility condition between a and g. To simplify the notation, from now on we will drop the tildes.

We will construct a unique solution of the problem in the class

$$H(a,c)=\{u: u-c+a\chi(\overline{\Omega^-})\in H_0^1(\Omega)\} \tag{7}$$

If $u\in H(a,c)$, then $[u]_\Gamma=a$ and $u|_{\partial\Omega}=g$. Note that $H_0^1(\Omega)$ can be identified with $H(0,0)$.

Definition 2.1. A function $u\in H(a,c)$ is a weak solution of Eq. (1)–(3), if $v=u-c+a\chi(\overline{\Omega^-})\in H_0^1(\Omega)$ satisfies

$$B[v,\psi]=F(\psi) \tag{8}$$

for all $\psi\in H_0^1(\Omega)$, where

$$B[v,\psi]=\int_{\Omega^+}\beta\bigtriangledown v\cdot\bigtriangledown\psi+\int_{\Omega^-}\beta\bigtriangledown v\cdot\bigtriangledown\psi \tag{9}$$

$$F(\psi)=\int_\Omega f\psi+\int_\Omega\beta\bigtriangledown c\cdot\bigtriangledown\psi+\int_{\Omega^-}\beta\bigtriangledown a\cdot\bigtriangledown\psi+\int_\Gamma b\psi \tag{10}$$

Or equivalently

Definition 2.2. A function $u\in H(a,c)$ is a weak solution of Eq. (1)–(3), if u satisfies, for all $\psi\in H_0^1(\Omega)$,

$$\int_{\Omega^+}\beta\bigtriangledown u\cdot\bigtriangledown\psi+\int_{\Omega^-}\beta\bigtriangledown u\cdot\bigtriangledown\psi=\int_\Omega f\psi+\int_\Gamma b\psi \tag{11}$$

A classical solution of Eq. (1)–(3), $u|_{\Omega^\pm}\in C^2(\overline{\Omega^\pm})$ is necessarily a weak solution. Because all the subdomains' boundaries $\partial\Omega^\pm$ are Lipschitz continuous, the integration by parts are legal in each subdomain, $\Omega^\pm$, see Theorem 1.5.3.1 in [10].

We have the following theorem:

Theorem 2.1. *If $f\in L^2(\Omega)$, and a, b, and $c\in H^1(\Omega)$, then there exists a unique weak solution of* Eq. (1)–(3) *in $H(a,c)$.*

Proof. See Theorem 2.1 in [4]. □

3. Numerical method

For ease of discussion in this section, and for accuracy testing in the next section, we assume that a, b and c are smooth on the closure of Ω, β and f are smooth on Ω^+ and Ω^-, but they may be discontinuous across the interface Γ. However, $\partial\Omega$, $\partial\Omega^-$ and $\partial\Omega^+$ are kept to be Lipschitz continuous. We assume that there is a Lipschitz continuous and piecewise smooth level-set function ϕ on Ω, where $\Gamma=\{\phi=0\}$, $\Omega^-=\{\phi<0\}$ and $\Omega^+=\{\phi>0\}$. A unit vector $n=\frac{\bigtriangledown\phi}{|\bigtriangledown\phi|}$ can be obtained on $\overline{\Omega}$, which is a unit normal vector of Γ at Γ pointing from Ω^- to Ω^+.

In this paper, we restrict ourselves to a rectangular domain $\Omega = (x_{min}, x_{max}) \times (y_{min}, y_{max})$ in the plane, and β is a 2×2 matrix that is uniformly elliptic in each subdomain. Given positive integers I and J, set $\Delta x = (x_{max} - x_{min})/I$ and $\Delta y = (y_{max} - y_{min})/J$. We define a uniform Cartesian grid $(x_i, y_j) = (x_{min} + i\Delta x, y_{min} + j\Delta y)$ for $i = 0, \ldots, I$ and $j = 0, \ldots, J$. Each (x_i, y_j) is called a grid point. For the case $i = 0, I$ or $j = 0, J$, a grid point is called a boundary point, otherwise it is called an interior point. The grid size is defined as $h = max(\Delta x, \Delta y) > 0$.

Two sets of grid functions are needed and they are denoted by

$$H^{1,h} = \{\omega^h = (\omega_{i,j}) : 0 \leqslant i \leqslant I, 0 \leqslant j \leqslant J\}$$

and

$$H_0^{1,h} = \{\omega^h = (\omega_{i,j}) \in H^{1,h} : \omega_{i,j} = 0 \text{ if } i = 0, I \text{ or } j = 0, J\}$$

We cut every rectangular region $[x_i, x_{i+1}] \times [y_j, y_{j+1}]$ into two pieces of right triangular regions: one is bounded by $x = x_i, y = y_j$ and $y = \frac{y_{j+1} - y_j}{x_i - x_{i+1}}(x - x_{i+1}) + y_j$, and the other is bounded by $x = x_{i+1}, y = y_{j+1}$ and $y = \frac{y_{j+1} - y_j}{x_i - x_{i+1}}(x - x_{i+1}) + y_j$. Collecting all those triangular regions, we obtain a uniform triangulation $T^h : \bigcup_{K \in T^h} K$, see Fig. 1. We can also choose the hypotenuse to be $y = \frac{y_{j+1} - y_j}{x_{i+1} - x_i}(x - x_i) + y_j$, and get another uniform triangulation from the same Cartesian grid. There is no conceptual difference for our method on these two triangulations.

If $\phi(x_i, y_j) \leqslant 0$, we count the grid point (x_i, y_j) as in $\overline{\Omega^-}$; otherwise we count it as in Ω^+. We call an edge (an edge of a triangle in the triangulation) an interface edge if two of its ends (vertices of triangles in the triangulation) belong to different subdomains; otherwise we call it a regular edge.

We call a cell K an interface cell if its vertices belong to different subdomains. In the interface cell, we write $K = K^+ \bigcup K^-$. K^+ and K^- are separated by a straight line segment, denoted by Γ_K^h. The two end points of the line segment Γ_K^h are located on the interface Γ and their locations can be calculated from the linear interpolations of the discrete level-set functions $\phi^h = \phi(x_i, y_j)$. The vertices of K^+ are located in $\Omega^+ \bigcup \Gamma$ and the vertices of K^- are located in $\Omega^- \bigcup \Gamma$. K^+ and K^- are approximations of the regions of $K \bigcap \Omega^+$ and $K \bigcap \Omega^-$, respectively. We call a cell K a regular cell if all its vertices belong to the same subdomain, either Ω^+ or Ω^-. For a regular cell, we also write $K = K^+ \bigcup K^-$, where $K^- = \{\}$ (empty set) if all vertices of K are in Ω^+, and $K^+ = \{\}$ if all vertices of K are in Ω^-. Clearly $\Gamma_K^h = \{\}$ in a regular cell, and K^+ and K^- are approximations of the regions $K \bigcap \Omega^+$ and $K \bigcap \Omega^-$, respectively. We use $|K^+|$ and $|K^-|$ to represent the areas of K^+ and K^-, respectively.

Two extension operators are needed. The first one is $T^h : H^{1,h} \rightarrow H_0^1(\Omega)$. For any $\psi^h \in H_0^{1,h}$, $T^h(\psi^h)$ is a standard continuous piecewise linear function, which is a linear function in every triangular cell and $T^h(\psi^h)$ matches ψ^h on grid points. Clearly such a function set, denoted by $H_0^{1,h}$, is a finite dimensional subspace of $H_0^1(\Omega)$. The second extension operator U^h is constructed as follows. For any $u^h \in H^{1,h}$ with $u^h = g^h$ at boundary points, $U^h(u^h)$ is a piecewise linear function and matches u^h on grid points. It is a linear function in each regular cell, just like the first extension operator $U^h(u^h) = T^h(u^h)$ in a regular cell. In each interface cell, it consists of two pieces of linear functions, one is on K^+ and the other is on K^-. The location of its discontinuity in the interface cell is the straight line segment Γ_K^h. Note that two end points of the line segment are located on the interface Γ, and hence the interface condition $[u] = a$ could be and is enforced exactly at these two end points. In each interface cell, the interface condition $[\beta \bigtriangledown u \cdot n] = b$ is enforced with the value b at the middle point of Γ_K^h. Clearly such a function is not continuous in general, and neither is the set of such functions a linear space. We denote the set of such functions as $H_{a,c}^{1,h}$, which should be thought as an approximation of the solution class $H(a, c)$ (see Eq. (7)) plus the restriction of $[\beta \bigtriangledown u \cdot n] = b$. Similar versions of such extension can be found in the literature [7,9]. In order to use this extension, we need the following theorem.

Theorem 3.1. *For all $u^h \in H^{1,h}, U^h(u^h)$ can be constructed uniquely, provided T^h, ϕ, a and b are given.*

Proof. There are three typical cases for $U^h(u^h)$.

Case 0. If K is a regular triangle, see Fig. 2, $U^h(u^h) = T^h(u^h)$, i.e.,

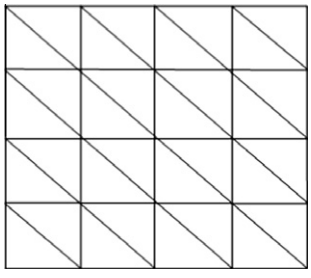

Fig. 1. A uniform triangulation.

$$U^h(u^h) = u(p_1) + \frac{u(p_2) - u(p_1)}{\triangle x}(x - x_i) + \frac{u(p_3) - u(p_1)}{\triangle y}(y - y_i) \tag{12}$$

Case 1. If K is an interface triangle, and the interface Γ is cutting through two legs of K, see Fig. 3, then

$$U^h(u^h) = \begin{cases} u(p_1) + u_x^+(x - x_i) + u_y^+(y - y_i)(x, y) \in K^+ \\ u(p_2) + u_x^-(x - x_i - \triangle x) + u_y^-(y - y_i)(x, y) \in K^- \end{cases} \tag{13}$$

Here $u_y^- = \frac{u(p_3) - u(p_2)}{\triangle y} + \frac{\triangle x}{\triangle y} u_x^-$. In Fig. 3, $\vec{n} = \left(-\frac{dy}{\sqrt{dx^2 + dy^2}}, -\frac{dx}{\sqrt{dx^2 + dy^2}} \right)$.

$$\begin{cases} u_x^+ = \frac{u(p_4) + a - u(p_1)}{dx} \\ u_y^+ = \frac{u(p_5) + a - u(p_1)}{dy} \end{cases} \tag{14}$$

In Fig. 4, we assume that the extensions of p_3p_5 and p_2p_4 intersect at a ghost point called p_1^G, therefore

$$\begin{cases} \frac{u(p_1^G) - u(p_4)}{dx} = \frac{u(p_4) - u(p_2)}{\triangle x - dx} \\ \frac{u(p_1^G) - u(p_5)}{dy} = \frac{u(p_1^G) - u(p_3)}{\triangle y} \end{cases} \tag{15}$$

and

$$\begin{cases} u_x^- = \frac{u(p_2) - u(p_4)}{\triangle x - dx} \\ u_y^- = \frac{u(p_3) - u(p_5)}{\triangle y - dy} \end{cases} \tag{16}$$

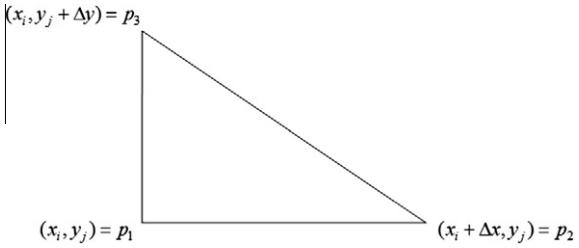

Fig. 2. Case 0: the regular cell.

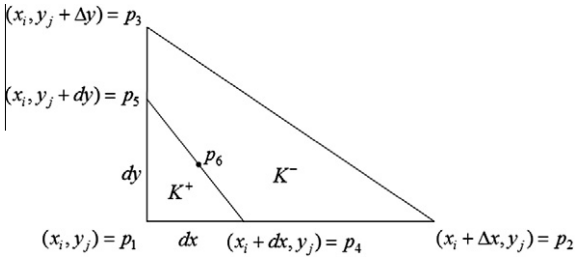

Fig. 3. Case 1: the interface cutting through two legs of a triangle.

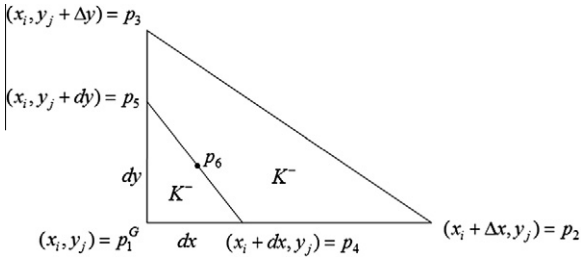

Fig. 4. Case 1: the ghost point.

From Eqs. (15) and (16), we can get

$$u(p_1^G) = \frac{dx}{\triangle x - dx}(u(p_4) - u(p_2)) + u(p_4) \tag{17}$$

$$u(p_5) = u(p_1^G) - \frac{dy}{\triangle y}(u(p_1^G) - u(p_3)) \tag{18}$$

Let

$$\beta = \begin{pmatrix} \beta_{11} & \beta_{12} \\ \beta_{21} & \beta_{22} \end{pmatrix} \tag{19}$$

From Eqs. (14)–(19), note that u_x^-, u_y^-, u_x^+ and u_y^+ can all be written as linear functions of $u(p_1), u(p_2), u(p_3)$ and $u(p_4)$. Since $b = \beta \bigtriangledown u \cdot \vec{n}$, we can obtain

$$\begin{aligned} b &= \beta^+ \bigtriangledown u^+ \cdot \vec{n} - \beta^- \bigtriangledown u^- \cdot \vec{n} \\ &= \beta_{11}^+ u_x^+ n_1 + \beta_{12}^+ u_y^+ n_1 + \beta_{21}^+ u_x^+ n_2 + \beta_{22}^+ u_y^+ n_2 - \left(\beta_{11}^- u_x^- n_1 + \beta_{12}^- u_y^- n_1 + \beta_{21}^- u_x^- n_2 + \beta_{22}^- u_y^- n_2\right) \end{aligned} \tag{20}$$

From Eqs. (14)–(20), we can obtain the value of $u(p_4)$. It is a linear function of $u(p_1), u(p_2), u(p_3)$. Hence u_x^-, u_y^-, u_x^+ and u_y^+ can be written in the following form

$$\begin{aligned} u_x^+ &= c_{x,1}^+ u(p_1) + c_{x,2}^+ u(p_2) + c_{x,3}^+ u(p_3) + c_{x,4}^+ a(p_4) + c_{x,5}^+ a(p_5) + c_{x,6}^+ b(p_6), \\ u_y^+ &= c_{y,1}^+ u(p_1) + c_{y,2}^+ u(p_2) + c_{y,3}^+ u(p_3) + c_{y,4}^+ a(p_4) + c_{y,5}^+ a(p_5) + c_{y,6}^+ b(p_6), \\ u_x^- &= c_{x,1}^- u(p_1) + c_{x,2}^- u(p_2) + c_{x,3}^- u(p_3) + c_{x,4}^- a(p_4) + c_{x,5}^- a(p_5) + c_{x,6}^- b(p_6), \\ u_y^- &= c_{y,1}^- u(p_1) + c_{y,2}^- u(p_2) + c_{y,3}^- u(p_3) + c_{y,4}^- a(p_4) + c_{y,5}^- a(p_5) + c_{y,6}^- b(p_6). \end{aligned} \tag{21}$$

To complete the proof, for Case 1, we need the following lemma: □

Lemma 3.1. *All coefficients c in* Eq. (21) *are finite and independent of u^h, a and b.*

Proof. From above discussion, it is easy to see that all coefficients c are independent of u^h, a and b.

Below we prove that $c_{x,3}^+$ is finite. The proofs for the other coefficients are similar.

$$c_{x,3}^+ = \alpha[-(\beta_{12}^+ dy + \beta_{22}^+ dx)dy(\triangle x - dx) + (\beta_{12}^- dy + \beta_{22}^- dx)dy(\triangle x - dx)] \tag{22}$$

where $\frac{1}{\alpha} = (\beta_{11}^+ dy + \beta_{21}^+ dx) \triangle y(\triangle x - dx)dy + (\beta_{12}^+ dy + \beta_{22}^+ dx) \triangle x(\triangle y - dy)dx + (\beta_{11}^- dy + \beta_{21}^- dx) \triangle y dx dy + (\beta_{12}^- dy + \beta_{22}^- dx) \triangle x dx dy$.

$c_{x,3}^+$ could be thought as a function of dx and dy. It is smooth on $[0, \triangle x] \times [0, \triangle y]$ except one point $(dx, dy) = (0,0)$. It is easy to see that if $dx = 0$ and $dy \neq 0$ or $dx \neq 0$ and $dy = 0$, $c_{x,3}^+ = 0$. Now denote $k = dy/dx \in (0, +\infty)$, and rewrite it as

$$c_{x,3}^+ = \alpha'\left[-(\beta_{12}^+ k + \beta_{22}^+)k(\triangle x - dx) + (\beta_{12}^- k + \beta_{22}^-)k(\triangle x - dx)\right] \tag{23}$$

where $\frac{1}{\alpha'} = (\beta_{11}^+ k + \beta_{21}^+) \triangle y(\triangle x - dx)k + (\beta_{12}^+ k + \beta_{22}^+) \triangle x(\triangle y - k dx) + (\beta_{11}^- k + \beta_{21}^-)k \triangle y dx + (\beta_{12}^- k + \beta_{22}^-)k \triangle x dx$

Let dx go to zero. Then

$$\begin{aligned} c_{x,3}^+ &= \frac{-(\beta_{12}^+ k + \beta_{22}^+)k + (\beta_{12}^- k + \beta_{22}^-)k}{(\beta_{11}^+ k + \beta_{21}^+)k \triangle y + (\beta_{12}^+ k + \beta_{22}^+) \triangle y} \\ &= \frac{-(\beta_{12}^+ k + \beta_{22}^+)k + (\beta_{12}^- k + \beta_{22}^-)k}{(k \quad 1)\begin{pmatrix} \beta_{11}^+ & \beta_{12}^+ \\ \beta_{21}^+ & \beta_{22}^+ \end{pmatrix}\begin{pmatrix} k \\ 1 \end{pmatrix} \triangle y} \end{aligned} \tag{24}$$

Since $\begin{pmatrix} \beta_{11}^+ & \beta_{12}^+ \\ \beta_{21}^+ & \beta_{22}^+ \end{pmatrix}$ is uniformly elliptic, the denominator is always positive. Further, both the numerator and the denominator are quadratic functions of k. For k going to infinity, the limit of the fraction is finite. Therefore, $c_{x,3}^+$ is finite.

Case 2. If K is an interface triangle, and the interface Γ is cutting through one leg and the hypotenuse of K, see Fig. 5, then

$$U^h(u^h) = \begin{cases} u(p_2) + u_x^+(x - x_i - \triangle x) + u_y^+(y - y_i)(x,y) \in K^+ \\ u(p_1) + u_x^-(x - x_i) + \frac{u(p_3) - u(p_1)}{\triangle y}(y - y_i)(x,y) \in K^- \end{cases} \tag{25}$$

Similar derivation as in Case 1 gives

$$\begin{aligned}
u_x^+ &= d_{x,1}^+ u(p_1) + d_{x,2}^+ u(p_2) + d_{x,3}^+ u(p_3) + d_{x,4}^+ a(p_4) + d_{x,5}^+ a(p_5) + d_{x,6}^+ b(p_6),\\
u_y^+ &= d_{y,1}^+ u(p_1) + d_{y,2}^+ u(p_2) + d_{y,3}^+ u(p_3) + d_{y,4}^+ a(p_4) + d_{y,5}^+ a(p_5) + d_{y,6}^+ b(p_6),\\
u_x^- &= d_{x,1}^- u(p_1) + d_{x,2}^- u(p_2) + d_{x,3}^- u(p_3) + d_{x,4}^- a(p_4) + d_{x,5}^- a(p_5) + d_{x,6}^- b(p_6),\\
u_y^- &= d_{y,1}^- u(p_1) + d_{y,2}^- u(p_2) + d_{y,3}^- u(p_3) + d_{y,4}^- a(p_4) + d_{y,5}^- a(p_5) + d_{y,6}^- b(p_6).
\end{aligned} \tag{26}$$

To complete the proof, for Case 2, we need the following lemma: □

Lemma 3.2. *All coefficients d in* Eq. (26) *are finite and independent of* u^h, *a and b.*

Proof. The proof is the same as the proof of Lemma 3.1, and is omitted here.

From the above discussion, we complete the proof of Theorem 3.1 and all coefficients c and d are independent of u^h, a and b. □

Based on the above discussion, we propose the following method:

Method 3.1 Find a discrete function $u^h \in H^{1,h}$ such that $u^h = g^h$ on boundary points and so that for all $\psi^h \in H_0^{1,h}$, we have

$$\sum_{K\in T^h}\left(\int_{K^+}\beta\bigtriangledown U^h(u^h)\cdot\bigtriangledown T^h(\psi^h)+\int_{K^-}\beta\bigtriangledown U^h(u^h)\cdot\bigtriangledown T^h(\psi^h)\right)=\sum_{K\in T^h}\left(\int_{K^+}fT^h(\psi^h)+\int_{K^-}fT^h(\psi^h)+\int_{\Gamma_K^h}bT^h(\psi^h)\right) \tag{27}$$

Note that $u = g$ on the boundary is the same as $u - c + a\chi(\overline{\Omega^-}) = 0$ on the boundary.

For the general case with $p \neq 0, q \neq 0$, integral for these lower order terms could be added to the above weak formulation.

To implement the above method, we use the Gaussian quadrature rule for integrals. The idea is illustrated in Fig. 6. If T is separated into two pieces by the interface $\overline{u_4u_5}$, we connect u_3 and u_4, then we get three triangles: $T_1 = \triangle u_1u_4u_5, T_2 = \triangle u_2u_3u_4, T_3 = \triangle u_3u_4u_5$. For each triangle, we label the center point p_{ij} of each edge $\overline{u_iu_j}$. In numerical computation, we apply the average of three $f(p_{ij})$ in each triangle. Numerical results show an improvement over [4], where fewer sample points were used.

Since our solution bases and test function bases are different, the matrix A for the linear system generated by Method 3.1 is not symmetric in the presence of an interface. However, we can prove it is positive definite.

Theorem 3.2. *If* β *is positive definite,* $p = q = 0$, *then the* $n \times n$ *matrix A for the linear system generated by Method 3.1 is positive definite.*

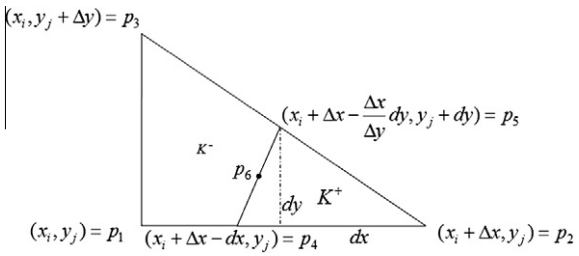

Fig. 5. Case 2: the interface cutting through a leg and a hypotenuse of a triangle.

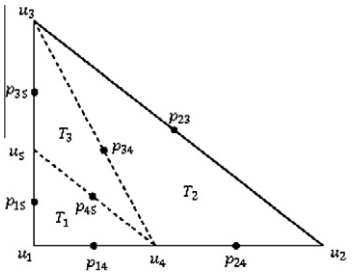

Fig. 6. Quadrature.

Proof. For any vector $c \in R^n$,

$$c^T A c = \sum_{i,j=1}^{n} a_{ij} c_i c_j = B\left[\sum_{i=1}^{n} c_i u^i, \sum_{i=1}^{n} c_i \psi^i\right]$$

where u^i and ψ^i are basis functions for the solution and the test function, respectively. Note that they have compact support and have nonzero values only inside the six triangles around the ith grid point. For ease of discussion, we decompose each of u^i and ψ^i into six parts, so that each part has nonzero values only inside one triangle. Now the summation over i is equivalent to a summation over all the triangles, and there are three terms, $c_1u_1 + c_2u_2 + c_3u_3$, $c_1\psi_1 + c_2\psi_2 + c_3\psi_3$ for each triangle, where $u_1,u_2,u_3,\psi_1,\psi_2,\psi_3$ equals 1 on one vertex of a triangle and zero on two other vertices. The difference between u_i and ψ_i is, u_i depends on the location of the interface and ψ_i does not. $c_1u_1 + c_2u_2 + c_3u_3$ is a piecewise linear function satisfying the jump conditions and $c_1\psi_1 + c_2\psi_2 + c_3\psi_3$ is a linear function. At the three vertices, the two functions coincide. Now we can set the jump conditions $a = 0$ and set b to have the value in the triangle such that $c_1u_1 + c_2u_2 + c_3u_3 = c_1\psi_1 + c_2\psi_2 + c_3\psi_3$ everywhere. In other words, we compensate for the jump in β by using b to make sure the gradients on both sides of the interface coincide. Since Lemmas 3.1 and 3.2 imply the matrix A is independent of a, b, choosing the above a, b would not change the matrix A and would only change the constant term, i.e., the right-hand side of the linear system. Now when we sum over all the triangles, we have

$$\sum_{i=1}^{n} c_i u^i = \sum_{i=1}^{n} c_i \psi^i$$

It now follows from the positive definiteness of β that

$$c^T A c = B\left[\sum_{i=1}^{n} c_i u^i, \sum_{i=1}^{n} c_i u^i\right] > 0$$

Therefore, A is positive definite. □

Remark 1. A positive definite matrix has positive determinant, and is therefore, invertible. It also has an LDM^T factorization where $D = diag(d_i)$ and $d_i > 0$ and L,M are lower triangular. The linear system $Ax = b$ can be solved efficiently.

Remark 2. For ease of discussion, we dropped both the p,q terms early. However, the Lax–Milgram Theorem, our Theorems 2.1 and 3.2 all work for the case $p = 0$ and $q > 0$ as well. For the case with nonzero p or negative q, the positive definiteness of A is no longer guaranteed, nor is one of the hypotheses of the Lax–Milgram Theroem.

4. Numerical experiments

Consider the problem

$$\begin{aligned}
&-\nabla\cdot(\beta\nabla u) + p\cdot\nabla u + qu = f, \text{ in } \Omega^{\pm},\\
&[u] = a, \text{ on } \Gamma,\\
&[(\beta\nabla u)\cdot n] = b, \text{ on } \Gamma,\\
&u = g, \text{ on } \partial\Omega,
\end{aligned}$$

on the rectangular domain $\Omega = (x_{min},x_{max}) \times (y_{min},y_{max})$. Γ is an interface and prescribed by the zero level-set $\{(x,y) \in \Omega \mid \phi(x,y) = 0\}$ of a level-set function $\phi(x,y)$. The unit normal vector of Γ is $n = \frac{\nabla\phi}{|\nabla\phi|}$ pointing from $\Omega^- = \{(x,y) \in \Omega \mid \phi(x,y) \leqslant 0\}$ to $\Omega^+ = \{(x,y) \in \Omega \mid \phi(x,y) \geqslant 0\}$.

In all numerical experiments below, the level-set function $\phi(x,y)$, the coefficients $\beta^{\pm}(x,y)$, $p^{\pm}(x,y)$, $q^{\pm}(x,y)$ and the solutions

$$\begin{aligned}
&u = u^+(x,y), \text{ in } \Omega^+,\\
&u = u^-(x,y), \text{ in } \Omega^-
\end{aligned}$$

are given. Hence

$$\begin{aligned}
&f = -\nabla\cdot(\beta\nabla u) + p\cdot\nabla u + qu,\\
&a = u^+ - u^-,\\
&b = (\beta^+\nabla u^+)\cdot n - (\beta^-\nabla u^-)\cdot n
\end{aligned}$$

on the whole domain Ω. g is obtained as a proper Dirichlet boundary condition, since the solutions are given.

All errors in solutions are measured in the L^∞ norm in the whole domain Ω. All errors in the gradients of solutions are measured in the L^∞ norm away from interfaces.

For Examples 1–10, we let $p(x,y) = q(x,y) = 0$ and we let $\beta^{\pm}$ be scalars. We implemented Method 3.1. For Example 11, $\beta^{\pm}$ are symmetric positive definite matrices, and we modified Method 3.1 by adding the integrals for lower order p,q terms. As we discussed in Section 2, in this general case, one of the hypotheses of the Lax–Milgram Theorem is not guaranteed. However, since we constructed the true solution first, the existence of a weak solution is automatically guaranteed. The numerical result is promising.

Examples 1–3 are taken from [19]. Compared with the result in [19], if the true solution does not have oscillation, as in Example 1, due to the elegant treatment in [19] for the sharp-edged interface, they obtained smaller error than ours for the same grid; however, as shown in Examples 2, 3, as the solution gets more oscillatory, our method is superior as we obtained better results than those presented in [19].

Example 1. The level-set function ϕ, the coefficients $\beta^{\pm}$ and the solution $u^{\pm}$ are given as follows:

$$\begin{aligned}
&\phi(r,\theta) = \frac{R\sin(\theta_t/2)}{\sin(\theta_t/2+\theta-\theta_r-2\pi(i-1)/5)} - r\\
&\theta_r + \pi(2i-2)/5 \leqslant \theta < \theta_r + \pi(2i-1)/5,\\
&\phi(r,\theta) = \frac{R\sin(\theta_t/2)}{\sin(\theta_t/2-\theta+\theta_r-2\pi(i-1)/5)} - r\\
&\theta_r + \pi(2i-3)/5 \leqslant \theta < \theta_r + \pi(2i-2)/5,
\end{aligned}$$

with $\theta_t = \pi/5$, $\theta_r = \pi/7$, $R = 6/7$ and $i = 1,2,3,4,5$.

$$\begin{aligned}
&\beta^+(x,y) = 1,\\
&\beta^-(x,y) = 2+\sin(x+y),\\
&u^+(x,y) = 8,\\
&u^-(x,y) = x^2+y^2+\sin(x+y)
\end{aligned}$$

Fig. 7 shows the numerical solution with our method using 40 grid points in both x and y directions. Table 1 shows the error on different grids.

Example 2. The level-set function ϕ is the same as in Example 1, the coefficients $\beta^{\pm}$ and the solution $u^{\pm}$ are given as follows:

$$\begin{aligned}
&\beta^+(x,y) = 1,\\
&\beta^-(x,y) = 2+\sin(x+y),\\
&u^+(x,y) = 6+\sin(2\pi x)\sin(2\pi y),\\
&u^-(x,y) = x^2+y^2+\sin(x+y)
\end{aligned}$$

Fig. 8 shows the numerical solution with our method using 40 grid points in both x and y directions. Table 2 shows the error on different grids.

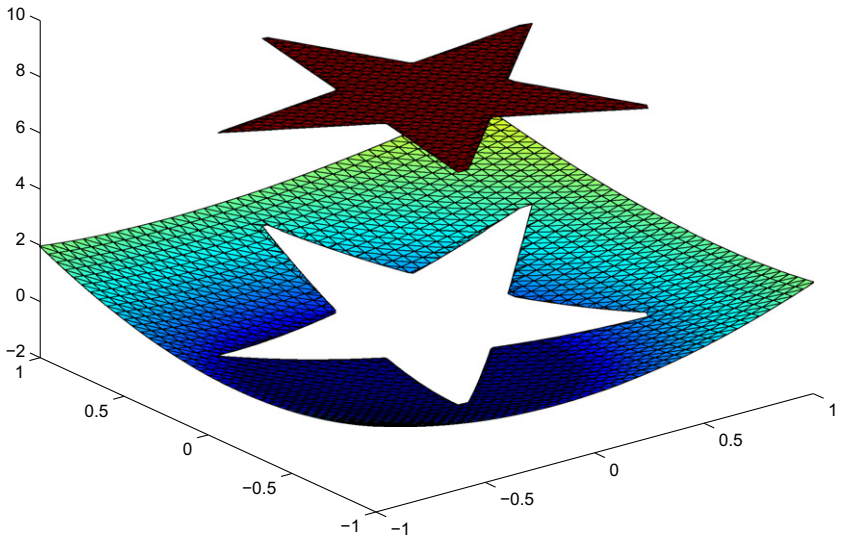

Fig. 7. Star: Case 1.

Table 1
Star: Case 1.

$n_x \times n_y$	Err in U	Order
20×20	4.082e-3	
40×40	1.135e-3	1.8466
80×80	3.12e-4	1.8631
160×160	8.4e-5	1.8931

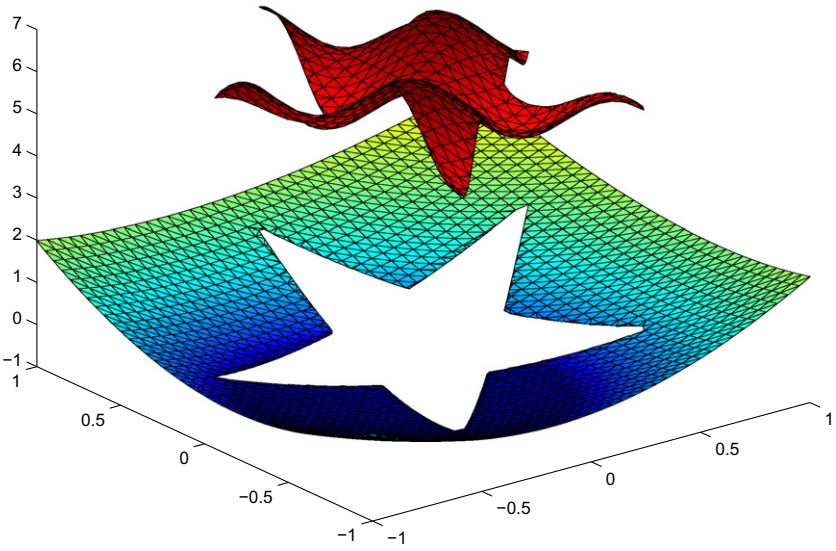

Fig. 8. Star: Case 2.

Table 2
Star: Case 2.

$n_x \times n_y$	Err in U	Order
20×20	4.054e-2	
40×40	1.058e-2	1.9380
80×80	2.496e-3	2.0836
160×160	6.31e-4	1.9839

Example 3. The level-set function ϕ is the same as in Example 1, the coefficients $\beta^{\pm}$ and the solution $u^{\pm}$ are given as follows:

$$\beta^+(x,y) = 1,$$
$$\beta^-(x,y) = 2 + \sin(x+y),$$
$$u^+(x,y) = 6 + \sin(6\pi x)\sin(6\pi y),$$
$$u^-(x,y) = x^2 + y^2 + \sin(x+y)$$

Fig. 9 shows the numerical solution with our method using 40 grid points in both x and y directions. Table 3 shows the error on different grids.

Example 4. This example is from [4], and our solution is more accurate than the previous work due to the quadrature rule discussed in Section 3. The level-set function ϕ, the coefficients $\beta^{\pm}$ and the solution $u^{\pm}$ are given as follows:

$$\phi(x,y) = (\sin(5\pi x) - y)(-\sin(5\pi y) - x),$$
$$\beta^+(x,y) = xy + 2,$$
$$\beta^-(x,y) = x^2 - y^2 + 3,$$
$$u^+(x,y) = 4 - x^2 - y^2,$$
$$u^-(x,y) = x^2 + y^2$$

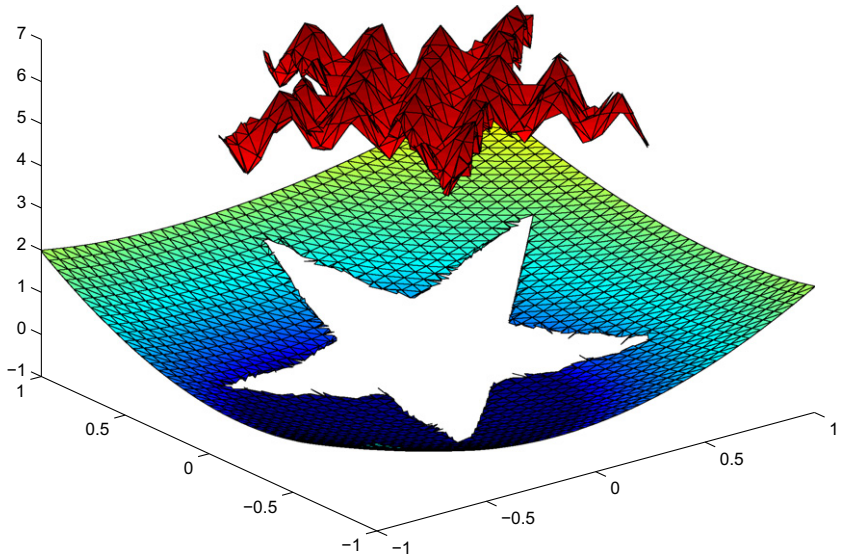

Fig. 9. Star: Case 3.

Table 3
Star: Case 3.

$n_x \times n_y$	Err in U	Order
20×20	3.402e-1	
40×40	8.879e-2	1.9379
80×80	2.331e-2	1.9294
160×160	5.675e-3	2.0383

Fig. 10 shows the numerical solution of the method using 40 grid points in both x and y directions. Table 4 shows the error on different grids. Compared with [4], we improved the order of accuracy from 0.8th order to close to second order, and for the same grid size, the error of our method is significantly smaller.

Examples 5–10 are taken from [4]. We use these six cases to investigate the order of the error in u and ∇u on solutions and interfaces with different regularity.

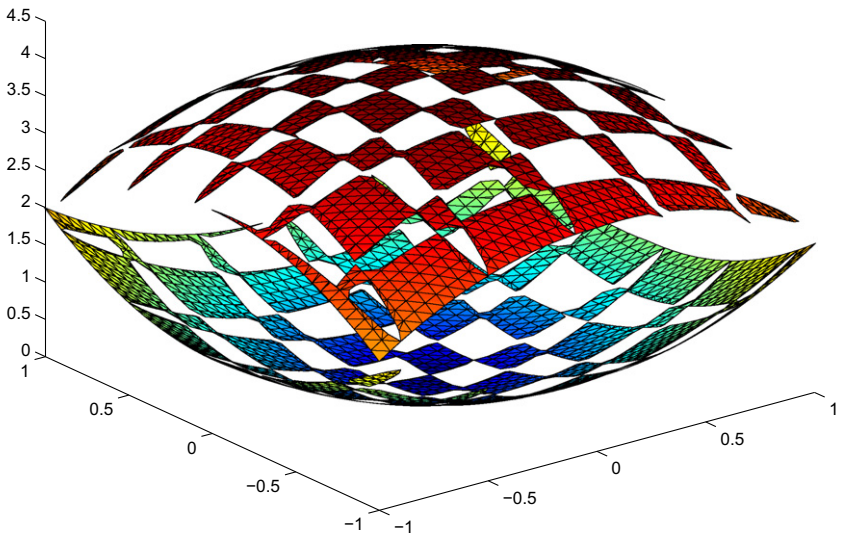

Fig. 10. Chess board.

Table 4
Chess board.

$n_x \times n_y$	Err in U	Order	Err in ∇U	Order
40×40	9.74e-4		4.650e-3	
80×80	2.71e-4	1.8051	3.454e-3	0.4290
160×160	9.4e-5	1.5276	1.433e-3	1.2692
320×320	2.6e-5	1.8541	6.89e-4	1.0565
41×39	9.36e-4		5.356e-3	
81×79	2.58e-4	1.8591	3.144e-3	0.7686
161×159	7.7e-5	1.7444	1.390e-3	1.1775
321×319	2.2e-5	1.8074	6.47e-4	1.1032

Example 5. The level-set function ϕ, the coefficients $\beta^{\pm}$ and the solution $u^{\pm}$ are given as follows. The interface is C^1 but not C^2 and u is C^2 but not C^3:

$$\phi(x,y) = y - 2x, x + y > 0$$
$$\phi(x,y) = y - (2x + x^2), x + y \leqslant 0$$
$$\beta^+(x,y) = (xy + 2)/5,$$
$$\beta^-(x,y) = (x^2 - y^2 + 3)/7,$$
$$u^+(x,y) = 2,$$
$$u^-(x,y) = \sin(x + y), x + y \leqslant 0$$
$$u^-(x,y) = x + y, x + y > 0$$

Fig. 11 shows the numerical solution with our method using a 41×39 grid. Table 5 shows the error on different grids.

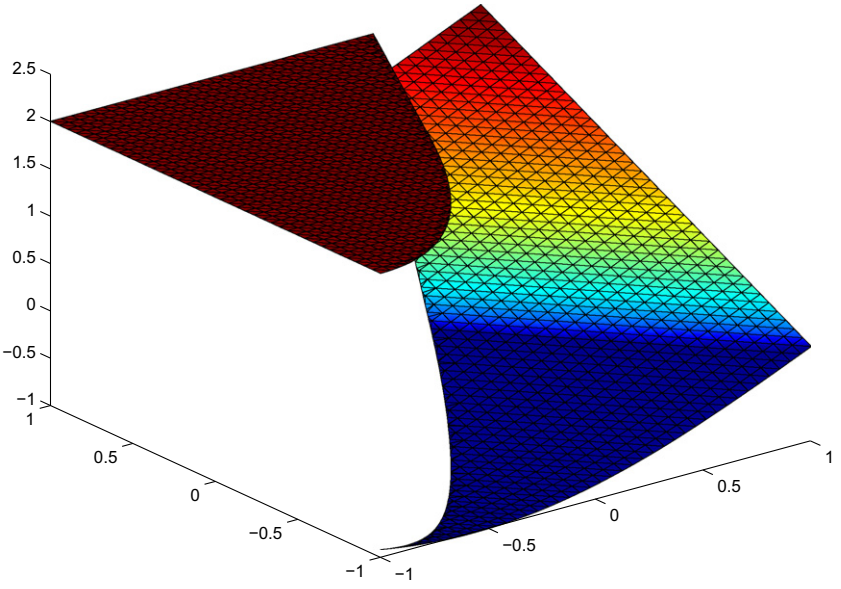

Fig. 11. Interface is C^1 but not C^2 and u is C^2 but not C^3.

Table 5
About second order in u and first order in ∇u.

$n_x \times n_y$	Err in U	Order	Err in ∇U	Order
41×39	1.18e-4		6.614e-4	
81×79	3.5e-5	1.7534	3.77e-4	0.8101
161×159	1.0e-5	1.8074	2.17e-4	0.7969
321×319	2.0e-6	2.3219	1.18e-4	0.8789

Example 6. The level-set function ϕ, the coefficients $\beta^{\pm}$ and the solution $u^{\pm}$ are given as follows. The interface is C^1 but not C^2 and u^- is piecewise C^1:

$$\phi(x,y) = y - 2x, x + y > 0$$
$$\phi(x,y) = y - (2x + x^2), x + y \leqslant 0$$
$$\beta^+(x,y) = (xy + 2)/5,$$
$$\beta^-(x,y) = (x^2 - y^2 + 3)/7,$$
$$u^+(x,y) = 2,$$
$$u^-(x,y) = \sin(x + y) + \cos(x + y), x + y \leqslant 0$$
$$u^-(x,y) = x + y + 1, x + y > 0$$

Fig. 12 shows the numerical solution with our method using a 41×39 grid. Table 6 shows the error on different grids.

Example 7. The level-set function ϕ, the coefficients $\beta^{\pm}$ and the solution $u^{\pm}$ are given as follows. The interface is C^1 but not C^2 and u is piecewise H^2:

$$\phi(x,y) = y - 2x, x + y > 0$$
$$\phi(x,y) = y - (2x + x^2), x + y \leqslant 0$$
$$\beta^+(x,y) = 1,$$
$$\beta^-(x,y) = 2 + \sin(x + y),$$
$$u^+(x,y) = 8,$$
$$u^-(x,y) = (x^2 + y^2)^{5/6} + \sin(x + y)$$

Fig. 13 shows the numerical solution with our method using an 81×41 grid. Table 7 shows the error on different grids.

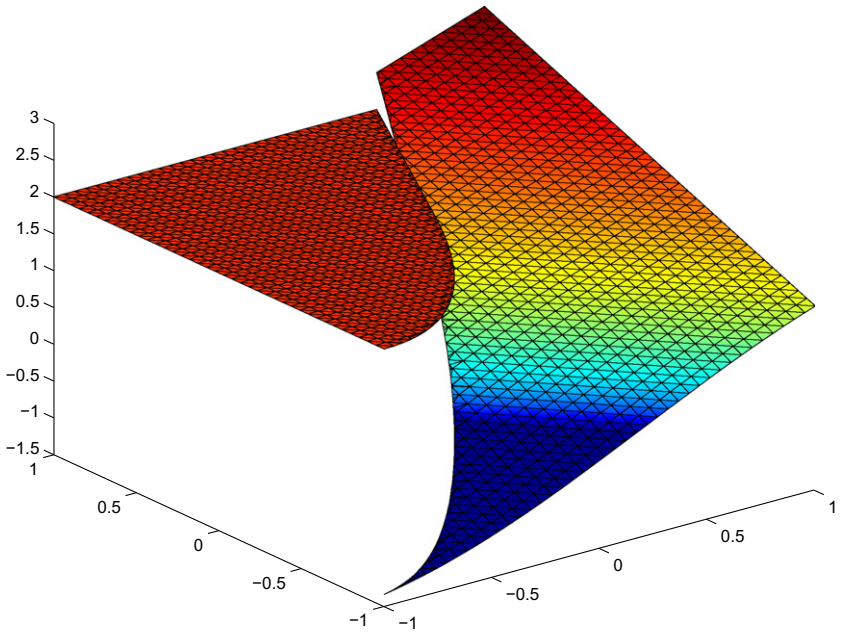

Fig. 12. Interface is C^1 but not C^2 and u^- is piecewise C^1.

Table 6
About first order in u and 0.8th order in ∇u.

$n_x \times n_y$	Err in U	Order	Err in ∇U	Order
41×39	1.169e-3		1.574e-2	
81×79	6.03e-4	0.9550	8.703e-3	0.8549
161×159	3.07e-4	0.9739	5.572e-3	0.6433
321×319	1.55e-4	0.9860	3.412e-3	0.7076

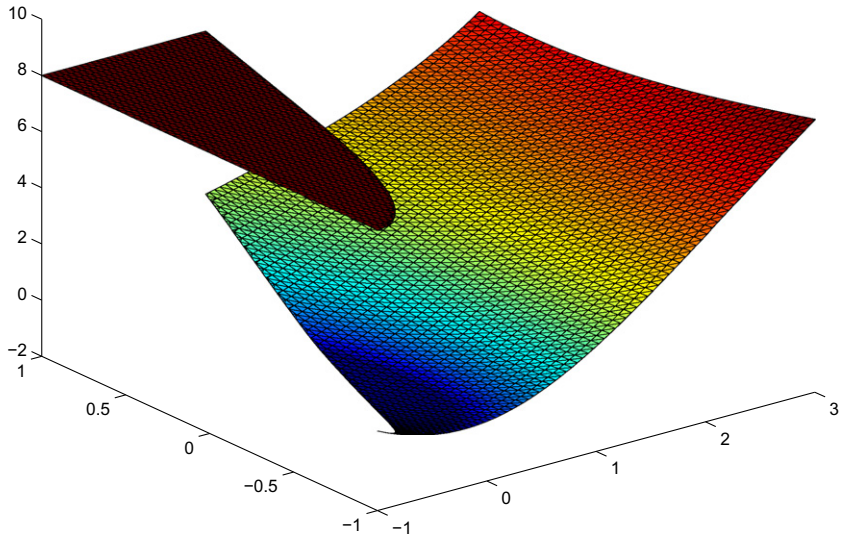

Fig. 13. Interface is C^1 but not C^2 and u is piecewise H^2 and has a singular point at (0,0).

Table 7
About 1.6th order in u and 0.65th order in ∇u.

$n_x \times n_y$	Err in U	Order	Err in ∇U	Order
81×41	1.255e-3		1.280e-2	
161×81	3.99e-4	1.6532	7.945e-3	0.6880
321×161	1.30e-4	1.6179	4.976e-3	0.6751

Example 8. The level-set function ϕ, the coefficients $\beta^{\pm}$ and the solution $u^{\pm}$ are given as follows. The interface is Lipschitz continuous and it has a kink at (0,0), u is piecewise C^2:

$$\begin{aligned}
&\phi(x,y) = y - 2x, x + y > 0\\
&\phi(x,y) = y + x/2, x + y \leqslant 0\\
&\beta^+(x,y) = (xy + 2)/5,\\
&\beta^-(x,y) = (x^2 - y^2 + 3)/7,\\
&u^+(x,y) = 8,\\
&u^-(x,y) = \sin(x + y), x + y \leqslant 0\\
&u^-(x,y) = x + y, x + y > 0
\end{aligned}$$

Fig. 14 shows the numerical solution with our method using an 81×41 grid. Table 7 shows the error on different grids.

Example 9. The level-set function ϕ, the coefficients $\beta^{\pm}$ and the solution $u^{\pm}$ are given as follows. The interface is Lipschitz continuous and it has a kink at (0,0), u is piecewise C^1:

$$\begin{aligned}
&\phi(x,y) = y - 2x, x + y > 0\\
&\phi(x,y) = y + x/2, x + y \leqslant 0\\
&\beta^+(x,y) = (xy + 2)/5,\\
&\beta^-(x,y) = (x^2 - y^2 + 3)/7,\\
&u^+(x,y) = 8,\\
&u^-(x,y) = \sin(x + y) + \cos(x + y), x + y \leqslant 0\\
&u^-(x,y) = x + y + 1, x + y > 0
\end{aligned}$$

Fig. 15 shows the numerical solution with our method using an 81×41 grid. Table 9 shows the error on different grids.

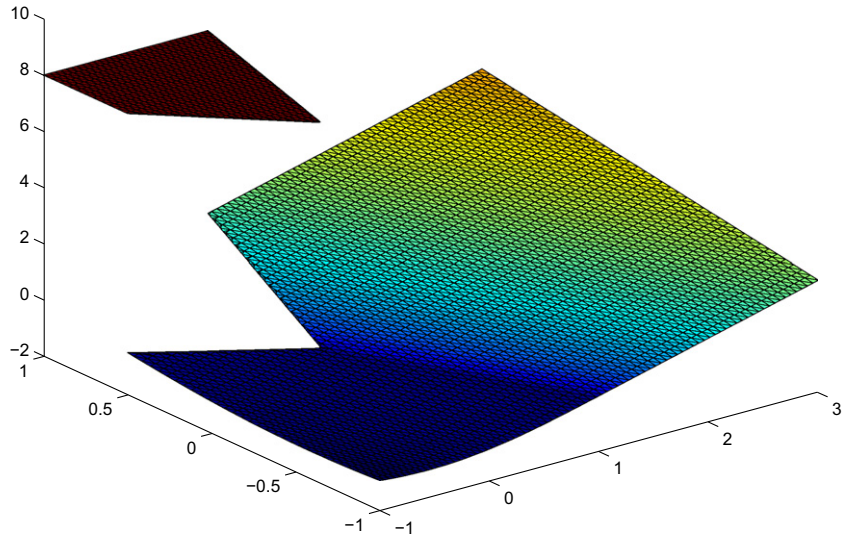

Fig. 14. Interface is Lipschitz continuous and it has a kink at (0,0), u is piecewise C^2.

Example 10. The level-set function ϕ, the coefficients $\beta^{\pm}$ and the solution $u^{\pm}$ are given as follows. The interface is Lipschitz continuous and it has a kink at (0,0), u is piecewise H^2:

$$\phi(x,y) = y - 2x, \ x + y > 0$$
$$\phi(x,y) = y + x/2, \ x + y \leqslant 0$$
$$\beta^+(x,y) = 1,$$
$$\beta^-(x,y) = 2 + \sin(x+y),$$
$$u^+(x,y) = 8,$$
$$u^-(x,y) = (x^2+y^2)^{5/6} + \sin(x+y)$$

Fig. 16 shows the numerical solution with our method using an 81×41 grid. Table 10 shows the error on different grids.

From Tables 6–10 we conclude the order of the error in u and ∇u, listed in Table 11

Compared with [4], when Γ is C^1, our order of accuracy is consistent with [4], and when Γ is Lipschitz continuous, our order of accuracy is higher than [4]. Besides, for the same grid size, our error is consistently smaller than [4], thanks to our more elegant quadrature formula discussed in Section 3.

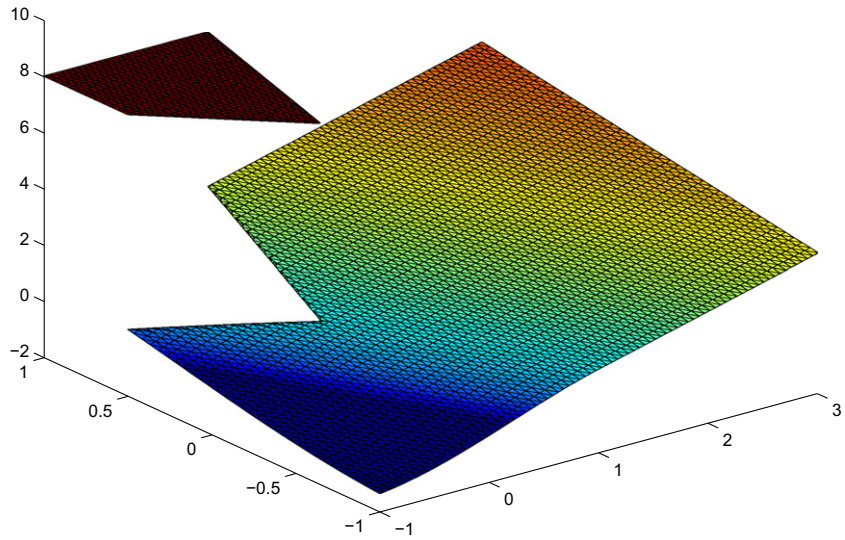

Fig. 15. Interface is Lipschitz continuous and it has a kink at (0,0), u is piecewise C^1.

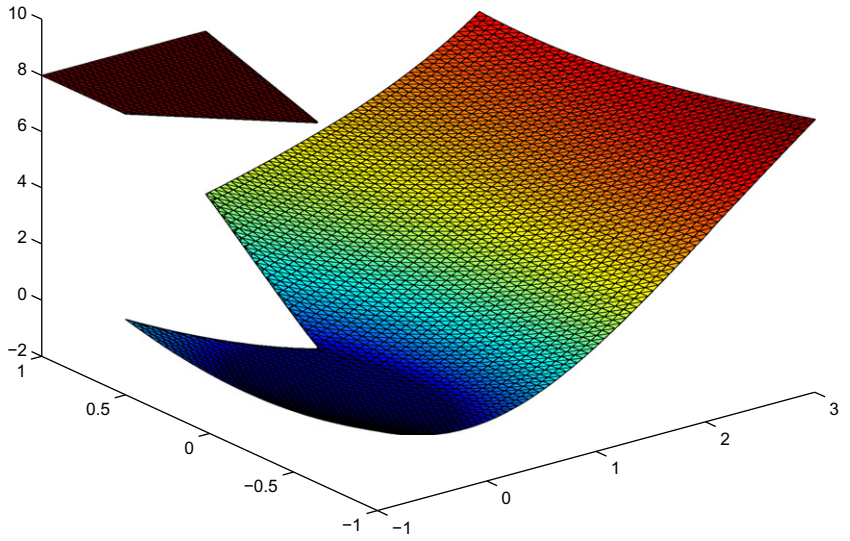

Fig. 16. Interface is Lipschitz continuous and it has a kink at (0,0), u is piecewise H^2, and has a singular point at (0,0).

Table 8
About 2nd order in u and 1st order in ∇u.

$n_x \times n_y$	Err in U	Order	Err in ∇U	Order
81 × 41	3.7e-5		5.79e-4	
161 × 81	1.0e-5	1.8875	1.76e-4	1.7180
321 × 161	3.0e-6	1.7370	9.2e-5	0.9359

Table 9
About first order in u and 0.7th order in ∇u.

$n_x \times n_y$	Err in U	Order	Err in ∇U	Order
41 × 21	7.166e-3		3.036e-2	
81 × 41	3.757e-3	0.9316	2.031e-2	0.5800
161 × 81	1.922e-3	0.9670	1.244e-2	0.7072
321 × 161	9.73e-4	0.9821	7.270e-3	0.7750

Table 10
About 1.5th order in u and 0.65th order in ∇u.

$n_x \times n_y$	Err in U	Order	Err in ∇U	Order
41 × 21	4.940e-3		4.698e-2	
81 × 41	1.745e-3	1.5013	2.978e-2	0.6577
161 × 81	6.06e-4	1.5258	1.886e-2	0.6590
321 × 161	2.09e-4	1.5358	1.194e-2	0.6595

Table 11
Conclusion of numerical experiments.

	Γ is C^1	Γ is Lipschitz continuous
u is C^2	2nd order in u and 1st order in ∇u	2nd order in u and 1st order in ∇u
u is C^1	1st order in u and 0.8th order in ∇u	1st order in u and 0.7th order in ∇u
u is H^2	1.6th order in u and 0.65th order in ∇u	1.5th order in u and 0.65th order in ∇u

Example 11. Our final example is a "happy face" interface and matrix form $\beta^{\pm}$, with lower order terms p,q present. The level-set function $\phi(x,y)$, the coefficients $\beta^{\pm}(x,y)$, $p^{\pm}(x,y)$, $q^{\pm}(x,y)$ and the solution $u^{\pm}(x,y)$ are given as follows:

$$\phi(x,y) = \max(\min(\phi_1,\phi_2,\phi_3),\phi_4,\phi_5,\phi_6,\min(\phi_7,\phi_8)),$$
$$\phi_1(x,y) = x^2 + y^2 - 0.75^2 - 0.15^2,$$
$$\phi_2(x,y) = (x-0.75)^2 + y^2 - 0.15^2,$$
$$\phi_3(x,y) = (x+0.75)^2 + y^2 - 0.15^2,$$
$$\phi_4(x,y) = -\frac{0.1}{0.12}(x-0.2)^2 - \frac{0.12}{0.1}(y-0.22)^2 + 0.12\cdot 0.1,$$
$$\phi_5(x,y) = -\frac{0.1}{0.12}(x+0.2)^2 - \frac{0.12}{0.1}(y-0.22)^2 + 0.12\cdot 0.1,$$
$$\phi_6(x,y) = -x^2 - (y+0.08)^2 + 0.12^2,$$
$$\phi_7(x,y) = -x^2 - (y+0.625)^2 + 0.425^2,$$
$$\phi_8(x,y) = -x^2 - (y+0.25)^2 + 0.2^2,$$
$$\beta^+(x,y) = \begin{pmatrix} xy+2 & xy+1 \\ xy+1 & xy+3 \end{pmatrix},$$
$$\beta^-(x,y) = \begin{pmatrix} x^2-y^2+3 & x^2-y^2+1 \\ x^2-y^2+1 & x^2-y^2+4 \end{pmatrix},$$
$$p^+(x,y) = \begin{pmatrix} xy \\ x^2-y^2-1 \end{pmatrix},$$
$$p^-(x,y) = \begin{pmatrix} x^2-y^2 \\ 2xy-1 \end{pmatrix},$$
$$q^+(x,y) = x^2 + y^2 - 2,$$
$$q^-(x,y) = xy + 1,$$
$$u^+(x,y) = 5 - 5x^2 - 5y^2,$$
$$u^-(x,y) = 7x^2 + 7y^2 + 1$$

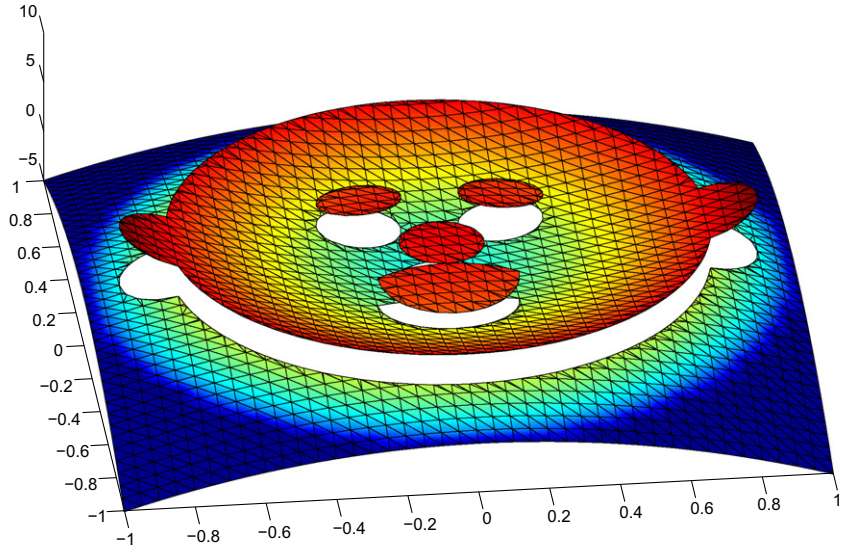

Fig. 17. Happy face.

Table 12
Happy face.

$n_x \times n_y$	Err in U	Order	Err in ∇U	Order
40×40	5.931e-3		5.121e-2	
80×80	1.669e-3	1.8293	2.757e-2	0.8933
160×160	4.51e-4	1.8878	1.686e-2	0.7095
320×320	1.24e-4	1.8628	8.940e-3	0.9153

Fig. 17 shows the numerical solution with our method using a 41×41 grid. Table 12 shows the error on different grids. The numerical result shows second order accuracy in the L^∞ norm for the solution and first order accuracy in the L^∞ norm for the gradient.

5. Conclusion

In this paper, we generalized the previous work in [4] to solve matrix coefficient second order elliptic equations with lower order terms present (see Example 11) for interface problems. We provided proofs for the generalized version of theorems in [4]. We also proved that the matrix for the linear system generated by our method is positive definite (but not symmetric). Through numerical experiments, our method achieved second order accuracy in the L^∞ norm, and we can handle the difficulties of sharp-edged interfaces and oscillatory solutions. Compared with the previous work in [4], we improved the order of accuracy for sharp-edged interfaces from 0.8th to close to second order, see Example 4. Compared with the result in [19], the more oscillatory the solution is, the more advantageous our method is, see Examples 1–3. The orders of accuracy for solutions and interfaces of different regularity are listed in Table 11.

Acknowledgement

This research is partially supported by Louisiana Board of Regents RCS Grant No. LEQSF (2008–11)-RD-A-18.

References

[1] Lawrence C. Evans, Partial Differential Equations, American Mathematical Society, 1998.
[2] R. Fedkiw, T. Aslam, B. Merriman, S. Osher, A non-oscillatory eulerian approach to interfaces in multimaterial flows (the ghost fluid method), J. Comput. Phys. 152 (2) (1999) 457C492.
[3] P. Grisvard, Elliptic problems in nonsmooth domains – monographs and studies in mathematics. Pitman Advanced Publishing Program, ISSN 0743-0329, 1985.
[4] Songming Hou, Xu-Dong Liu, A numerical method for solving variable coefficient elliptic equations with interfaces, J. Comput. Phys. 202 (2005) 411–445.
[5] R.J. LeVeque, Z. Li, The immersed interface method for elliptic equations with discontinuous coefficients and singular sources, SIAM J. Numer. Anal. 31 (1994) 1019.
[6] Z. Li, A fast iterative algorithm for elliptic interface problems, SIAM J. Numer. Anal. 35 (1) (1998) 230C254.
[7] Z. Li, T. Lin, X. Wu, New cartesian grid methods for interface problems using the finite element formulation, Numerische Mathematik, 9661–98: Preprint. NCSU CRSC–TR99–12, 2003.
[8] Zhilin Li, Kazufumi Ito, The Immersed Interface Method: Numerical Solutions of Pdes Involving Interfaces and Irregular Domains, SIAM, Philadelphia, 2006.
[9] Xu-Dong Liu, Ronald P. Fedkiw, Myungjoo Kang, A boundary condition capturing method for Poisson's equation on irregular domains, J. Comput. Phys. 160 (1) (2000) 151C178.
[10] Xu-Dong Liu, T. Sideris, Convergence of the ghost fluid method for elliptic equations with interfaces, Math. Comp. 72 (2003).
[11] A. Mayo, The fast solution of Poisson's and biharmonic equations in irregular domains, SIAM J. Numer. Anal. 21 (2) (1984) 285C299.
[12] A. Mayo, Fast high order accurate solutions of Laplace's equation on irregular domains, SIAM J. Sci. Stat. Comput. 6 (1) (1985) 144C157.
[13] J. Necas, Introduction to the theory of nonlinear elliptic equations, Teubner-Texte zur Mathematik, Band 52, ISSN 0138-502X, 1983.
[14] C. Peskin, Numerical analysis of blood flow in the heart, J. Comput. Phys. 25 (1977) 220C252.
[15] C. Peskin, B. Printz, Improved volume conservation in the computation of flows with immersed elastic boundaries, J. Comput. Phys. 105 (1993) 33C46.
[16] M. Sussman, P. Smereka, S. Osher, A level set approach for computing solutions to incompressible two-phase flow, J. Comput. Phys. 114 (1994) 146C154.
[17] Justin W.L. Wan, Xu-Dong Liu, A boundary condition capturing multigrid approach to irregular boundary problems, SIAM J. Sci. Comput. 25 (6) (2004) 1982C2003.
[18] W.-J. Ying, C.S. Henriquez, A kernel-free boundary integral method for elliptic boundary value problems, J. Comput. Phys. 227 (2) (2007) 1046–1074.
[19] Sining Yu, Yongcheng Zhou, G.W. Wei, Matched interface and boundary (MIB) method for elliptic problems with sharp-edged interfaces, J. Comput. Phys. 224 (2007) 729C756.
[20] Chen Zhiming, Zou Jun, Finite element methods and their convergence for elliptic and parabolic interface problems, Numerische Mathematik 79 (1998) 175C202.
[21] Y.C. Zhou, Shan Zhao, Michael Feig, G.W. Wei, High order matched interface and boundary method for elliptic equations with discontinuous coefficients and singular sources, J. Comput. Phys. 213 (2006) 1–30.
[22] P. Colella, H. Johansen, A Cartesian grid embedded boundary method for Poisson's equation on irregular domains, J. Comput. Phys. 60 (1998) 85C147.
[23] M. Oevermann, R. Klein, A Cartesian grid finite volume method for elliptic equations with variable coefficients and embedded interfaces, J. Comput. Phys. 219 (2006) 749C769.
[24] M. Oevermann, C. Scharfenberg, R. Klein, A sharp interface finite volume method for elliptic equations on Cartesian grids, J. Comput. Phys. 228 (2009) 5184C5206.
[25] Paul Macklin, John S. Lowengrub, A new ghost cell/level set method for moving boundary problems: application to tumor growth, J. Sci. Comput. 35 (2008) 266–299.